Available online at www.sciencedirect.com
ScienceDirect
Trans. Nonferrous Met. Soc. China 24(2014) 3274−3284
Transactions of Nonferrous Metals Society of China
www.tnmsc.cn

Effects of die geometry on non-equal channel lateral extrusion (NECLE) of AZ80 magnesium alloy

Faramarz FERESHTEH-SANIEE[1], Mohammad ASGARI[1], Mahmoud BARATI[2], Sayed Mahmoud PEZESHKI[1]

1. Mechanical Engineering Department, Faculty of Engineering, Bu-Ali Sina University, Hamedan, Iran;
2. Applied Mechanics Department, Faculty of Mechanical Engineering, K.N. Toosi University of Technology, Tehran, Iran

Received 13 November 2013; accepted 24 March 2014

Abstract: Non-equal channel lateral extrusion (NECLE) is a new process that can be used to attain higher grain refinement in comparison with equal channel lateral extrusion (ECLE). The die design for this process was numerically and experimentally studied. After finding a good correlation between the numerical and experimental results, more comprehensive FE analyses were carried out. Different die geometrical parameters were considered and their effects on the induced plastic strain, stress distribution, velocity field and forming load of the process were investigated. It was found that by this process with a suitable set of die geometrical parameters, higher induced effective strain and more homogeneous strain distribution could be achieved in comparison with ECLE operation.

Key words: magnesium alloy; non-equal channel lateral extrusion (NECLE); die geometry; homogeneity; arbitrary Lagrangian−Eulerian (ALE) method

1 Introduction

Extrusion is categorized as a bulk metal forming process. CHOI et al [1] claimed that based on the directions of the ram movement and material flow, the extrusion process is classified into three major types, namely forward, backward and lateral extrusion. The material flow direction in the lateral extrusion is perpendicular to the direction of punch movement. Because of severe plastic deformation, this type of process can be used for achieving a suitable grain refinement. The majority of recently introduced extrusion operations are categorized as lateral extrusion process. SEGAL et al [2] first introduced the equal channel lateral extrusion (ECLE) as a novel deformation technique to deform materials through a die with two channels equal in cross section and intersecting at a certain angle. ZUYAN et al [3] presented a new method, namely changing channel extrusion (CCE) by finite element simulation, which could decrease the tensile stress and increase the hydrostatic pressure in the workpiece. This process was good for the plastic deformation of low ductility materials. OHASHI and HAYASHI [4] developed lateral extrusion with a lost core (LELC) as a new bulging process of pipes and its application on pipes of A6063 aluminum alloy. They claimed that by LELC process the forming limit was improved drastically compared with plain hydrostatic bulge forming. TALEBANPOUR et al [5] introduced dual equal channel lateral extrusion (DECLE) as a new method of severe plastic deformation to refine grains of a bulk material. This method has some important advantages compared with ECLE, such as strains that are more intensive obtained per pass, and less power needed to transact the process. Nevertheless, they reported that less homogeneous strain per pass was seen in the case of DECLE. TÓTH et al [6] investigated AA2124 aluminum alloy processed by a new method, namely non-equal channel lateral extrusion (NECLE). In comparison with the same material processed by ECLE, a much finer microstructure was obtained in NECLE, showing that in this modified ECLE process the grain refinement process was more efficient.

The equal channel lateral extrusion (ECLE) process is also known as either equal channel angular pressing (ECAP) or equal channel angular extrusion (ECAE). Many researchers are interested in this process because of its simplicity and practical nature. Non-equal channel lateral extrusion is also a newly introduced process

Corresponding author: Faramarz FERESHTEH-SANIEE; Tel: +98-811-8292630; E-mail: ffsaniee@basu.ac.ir, ffsaniee@yahoo.com
DOI: 10.1016/S1003-6326(14)63467-1

which is similar to ECLE but with some differences. TÓTH et al [6] showed that the main difference between these processes is that the ECLE process has two equal inward and outward channels whereas the NECLE process involves a smaller size for the outward channel. The main advantage of this change in the die geometry is a significant extra plastic strain after the first pass of the latter operation, compared with the former one [6]. Therefore, it can be concluded that NECLE operation results in a higher grain refinement and plastic strain in comparison with a single-pass ECLE process. Therefore, NECLE would be advantageous for industrial and practical applications.

Geometrical parameters of the extrusion die have essential effects on the quality of the product, energy requirements and production efficiency. Several researchers studied the effects of these parameters on the strain distribution, strain homogeneity, microstructural evolutions and forming load of ECLE and extrusion processes. YOON et al [7] studied the effects of inhomogeneity factors on the deformation pattern of an ECAP process. They reported the optimum die corner angles as well as the strain-hardening exponent. HU et al [8] investigated the effects of die structure and frictional conditions on the ECLE process of AZ31 Mg alloy using an FE model together with experimental tests. ZHANG et al [9] analyzed the metal flow of hot extrusion operation of Al profiles using a numerical model.

Due to their high specific strength, good recyclability and weldability, magnesium alloys have attracted many scientists and industries during the last decade. The present work is concerned with the NECLE operation of AZ80 Mg alloy. With this regard, several NECLE experiments were conducted for validation of the numerical findings. Then, incorporating the flow curves and friction factor obtained from separate tests in the FE code (ABAQUS/Explicit), a deep numerical investigation was carried out relating the effects of geometrical parameters of the tool on the amount of plastic strain caused in the component and the required forming load and energy. A good agreement was found between the experimental and numerical results. Moreover, an appropriate selection of die geometrical parameters can result in a more homogeneous product and lower force and energy requirements.

2 FE simulation of NECLE process

A 3D ALE finite element model was constructed in ABAQUS/Explicit to simulate the NECLE process of AZ80 magnesium alloy and study the effects of the die geometry on the induced plastic strain and the required forming load for the process. The Abaqus/Explicit FE code along with the ALE method was used due to the complex deformation nature of the NECLE operation.

2.1 ALE formulation

Forming processes such as closed die forging, rolling and extrusion usually lead to severe plastic deformation of the workpiece and a non-homogeneous strain distribution. BELYTSCHKO et al [10] claimed that the updated Lagrangian formulation (UL) is usually employed for the FE simulation of these problems. In this formulation, the mesh is attached to the material, and moves with it. The advantage of this approach is that free surfaces are automatically followed. In addition, it is possible to consider a history dependent behavior of the material. However, in large deformations a drawback arises, and the shape of elements may become severely distorted, which results in a less accurate outcome or a precipitous end of the simulation. Therefore, a Lagrangian formulation is not always a suitable method for simulation of forming processes including large plastic deformation.

In spite of Lagrangian formulation, unmovable mesh and flow of material through this mesh are major characteristics of Eulerian formulation. Because of material flow through the mesh, the initial mesh remains undistorted and the simulation can be continued infinitely. Fluid dynamic problems are commonly formulated with Eulerian description. One disadvantage of the Eulerian formulation is that the free boundary tracking is hard to perform because the free boundaries do not completely coincide with the element edge.

To overcome the above-mentioned difficulties of Lagrangian and Eulerian approaches, a new alternative formulation, namely arbitrary Lagrangian Eulerian (ALE) method, has been developed to take the basic advantages of the classical formulations. In the ALE formulation, the FE mesh is neither attached to the material nor fixed in the space. Moreover, the concentration of the mesh in a specific region and the mesh distortion are controlled by a procedure. Therefore, it is possible to manage the path-dependent behavior of the material and the free surface conditions while maintaining the mesh suitability by using the ALE formulation.

The ALE-adaptive meshing based on the operator split technique together with ABAQUS/Explicit code is employed in this research. Each time increment during the solution is split into Lagrangian and Eulerian phases. In the Lagrangian phase the material effects are considered; furthermore, to complete the ALE step, the convective effects which are vanished in the Lagrangian step are taken into account for the Eulerian phase. The convective effects are resulted from the node relocation procedure while optimizing the distorted mesh. LEER [11] showed that a second order advection algorithm is involved in the utilized ALE formulation to transfer the state variables from the old mesh to the new one. In addition, BENSON [12] employed half-index shift method for the advection procedure of momentum.

2.2 Model description

HIBBITT [13] claimed that the ALE-adaptive meshing provides a significant advantage of converting mesh to a pure Eulerian or pure Lagrangian formulation or assigning a sliding motion to the mesh. Two different methods, namely transient and steady state techniques, which were used for simulation of NECLE process, are described in the following subsections.

2.2.1 Transient simulation (ALE adaptive mesh domain)

HIBBITT [13] showed that in this model, the punch and die were simulated as rigid parts, and the sample was considered the ALE adaptive mesh domain and the volumetric smoothing method was utilized for preventing mesh from distortion (see Fig. 1(a)). In this model, all boundaries of the workpiece were considered a sliding boundary region. In other words, in the tangential direction to the boundary region, the mesh is free to move but in the direction normal to the boundary region, it is constrained, so the mesh moves with the material. Therefore, a sliding boundary region can be assumed as a path for the mesh that moves independently on the material. The sliding boundaries are shown in Fig. 1.

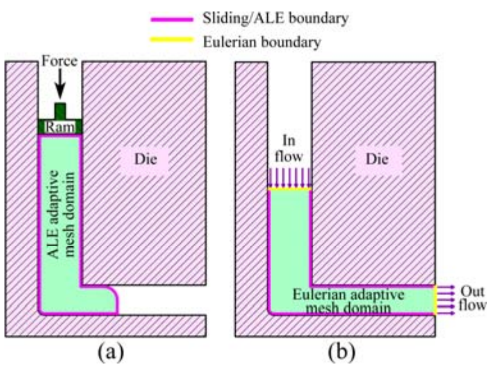

Fig. 1 ALE (a) and Eulerian (b) adaptive mesh domains

2.2.2 Steady-state simulation (Eulerian adaptive mesh domain)

Considering the load curve and the plastic strain distribution obtained based on the method explained in the previous section, it can be claimed that the NECLE process is steady state except for the initial stage of the deformation. Therefore, it can be modeled assuming a steady-state condition. PATIL-BASAVARAJ et al [14] stated that ECLE process could be considered a steady state as soon as the workpiece exited the deformation zone. In this research work, this assumption has been made, namely, the major field variables such as strain and stress have not changed with the time when the workpiece started leaving the deformation zone. With this regard, some forming operations were previously simulated as steady-state processes by different researchers. GOUVEIA et al [15] simulated forward extrusion process using steady-state FE analyses. They could accurately predict the load curve of the process employing a combined Eulerian−Lagrangian formulation. The flow pattern obtained based on an updated Lagrangian formulation was similar to that resulted from the ALE formulation.

In the present work, an Eulerian region was modeled assuming a steady-state condition. It is clear from Fig. 1(b) that the ram is not required to be simulated for this model. The material is drawn into the Eulerian region regarding inflow boundary and velocity boundary condition. After passing through the Eulerian region, the material exits through the outflow boundary.

In the transient model, a high-density mesh is required because of the sharp edges of the die. It is also necessary to prevent excessive distortion of the elements and input the material into the die surfaces. On the other hand, there is no distortion of the elements in a steady-state model. Moreover, the mesh is fixed in the steady-state model and, hence, a high-density mesh is not needed. Therefore, the CPU time for the transient model is much more than the steady-state one. In the steady-state simulation, the punch is not modeled, so the load curves are plotted against the time.

3 Experimental

3.1 Material and test samples

A cast AZ80 magnesium alloy was used as the material for performing the tests. The composition of this material is expressed in Table. 1. The NECLE test samples with dimensions of 15 mm (width)×15 mm (thickness)×80 mm (length) were produced using the machining process. The flow stress of this alloy was also determined using the cylindrical compression test. The compression tests were conducted at two different temperatures, namely 250 and 300 °C, and three strain rates, namely 0.001, 0.01 and 0.1 s^{-1}. The flow curves of the AZ80 magnesium alloy under these conditions are illustrated in Fig. 2. The flow curves of the material were inputted into the FE code to simulate the NECLE process.

3.2 Die geometry

The die was composed of two different channels, which were perpendicular to each other. The input channel width (P) was two times the output channel thickness (C). Two different dies with the extrusion ratios of P/C=1.5 and 2 were employed in this research. In an ECLE process the extrusion ratio is equal to 1.0

Table 1 Composition of AZ80 Mg alloy employed (mass fraction, %)

Al	Zn	Mn	Si	Cu
7.9	0.5	0.24	0.05	0.001

Fe	Ni	Other	Mg
0.002	0.001	0.1	Bal.

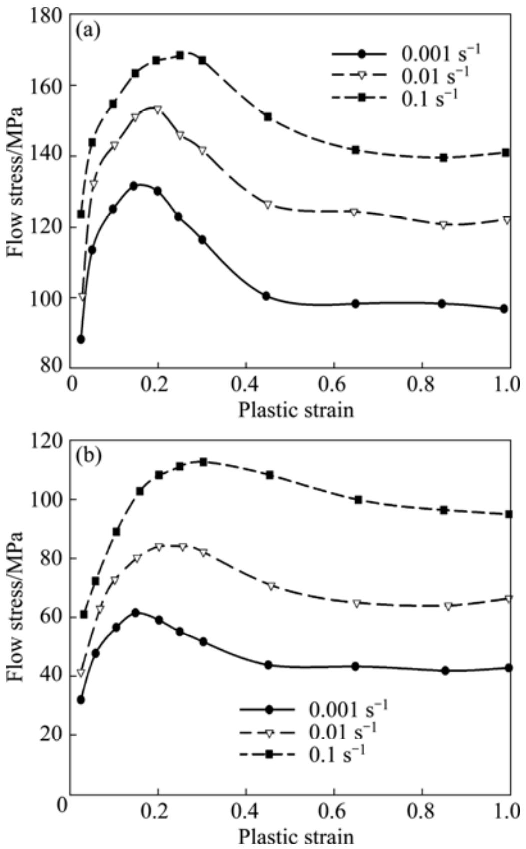

Fig. 2 Flow curves of AZ80 alloy at three different deformation rates and temperatures of 250 °C (a) and 300 °C (b) [16]

(P=C). Based on Fig. 3(a), r and R are the inner and outer corner radii, respectively. The employed die has the inner and outer corner radii of r=0 and R=4, and an inner corner angel of ϕ=90° (see Fig. 3(a)). The die set utilized for NECLE experimentation is shown in Fig. 3(b). Before manufacturing the die, several FE simulations were conducted to find a suitable set of geometrical parameters to achieve a homogeneous strain distribution after deformation. The aim was to obtain an optimized set of parameters for a die with P/C=2.

3.3 NECLE experiments

A 150 kN servo-electric testing machine was used for performing the experiments. The tests were conducted at temperatures of 250 and 300 °C and with constant ram velocities of 1 and 2 mm/min. As mentioned earlier, the NECLE process was conducted on two different extrusion ratios at each temperature. The details of NECLE experiments are demonstrated in Table 2. MoS_2 spray was used for lubrication of the surfaces of the die and sample. Also, to study the homogeneity of material's plastic deformation after NECLE process, the micro-hardness profile through the thickness of products' steady deformation zone was conducted by means of a Buehler Ltd-Lake Bluff-IL 60044 tester machine.

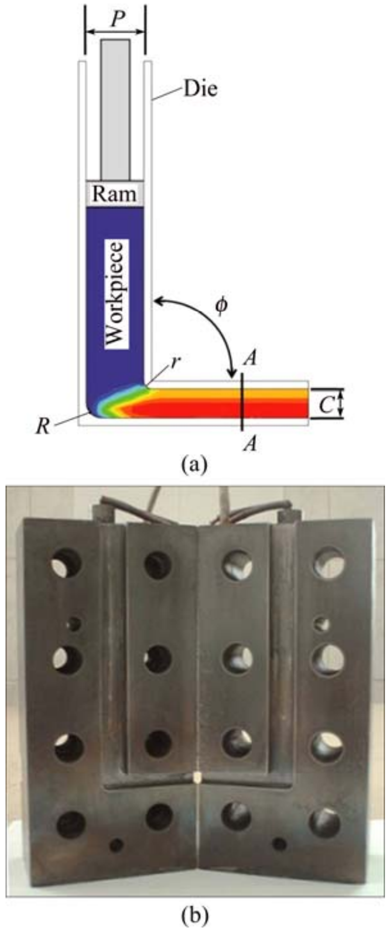

Fig. 3 Geometrical parameters of NECLE die (a) and die set (b) employed for conducting NECLE experiments

Table 2 Parameters of NECLE experiment

No.	P/C	Temperature/°C	Ram velocity/(mm·min^{-1})
1	2	250	1
2	2	250	2
3	2	300	2
4	1.5	250	2
5	1.5	300	2

4 Results and discussion

The effects of different parameters of the die on the plastic strain distribution in the extrusion direction and stress distribution in the deformation zone were studied by FE simulations. The geometrical parameters considered were the inner (r) and outer (R) radii, inner corner angle (ϕ) and extrusion ratio (P/C). Formation of the dead metal zone and its influence on the distribution of the effective strain were also studied. All the FE simulations were carried out using the flow behavior of AZ80 Mg alloy at 250 and 300 °C, constant ram velocities of 1 and 2 mm/min and a friction factor of μ=0.18 (with MoS_2 lubrication). The friction factor was obtained by the method explained by FERESHTEH-SANIEE et al [17]. They used new method and T-shape friction test to evaluate the friction factor. Coulomb friction law with a shear stress limitation was utilized for the FE simulations.

4.1 Effects of inner and outer die corner radii

In order to determine the effects of die corner radii on the deformation pattern of the NECLE process, dies with different corner radii were modeled. Nine FE models with various inner and outer die radii are summarized in Table. 3. The inner corner angle and the extrusion ratio for these FE analyses were ϕ=90° and P/C=2, respectively.

Table 3 Different values of inner (r) and outer (R) die radii

r/mm	R/mm
0	0
2	4
4	7

4.1.1 Effects of die outer radius

The effects of the die outer radius on the effective strain and stress distributions were investigated by maintaining the die inner radius constant (r=0). Three different die outer radii, namely R=0, 4 and 7 mm, were considered. The effective strain distributions obtained from these simulations are illustrated in Fig. 4. The smaller the die outer radius, the larger the induced effective strain. A maximum imposed effective strain of ε=2.42 is caused for R=0, which is approximately 75% larger than that of R=4 mm, with ε=1.38, and 94% higher than that with ε=1.25 for the die outer radius of R=7 mm. HU et al [8] reported a similar pattern for ECLE process. The formation of a dead-metal zone at the outer corner resulted in shear deformation in moving metal on the stable metal in the dead-zone. Hence, this might be the probable cause of larger strain values for R=0 in comparison with the other two R values. Therefore, the greater the outer radius of the NECLE die is, the lower the strain gradient is in the product, which means a more uniform mechanical behavior of the component. The imposed plastic strain at the outer radius was maintained through the horizontal channel. The effective von Mises stress distributions of the above-mentioned FE analyses are also shown in Fig. 5.

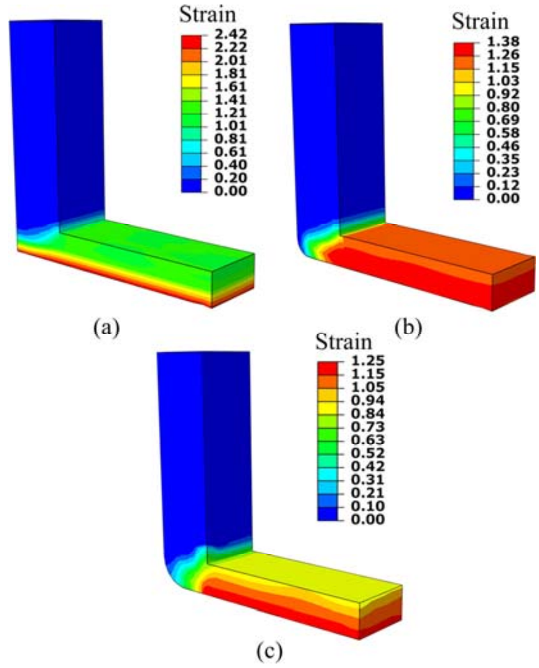

Fig. 4 Distributions of generalized plastic strain for r=0 and three different values of R: (a) R=0; (b) R=4 mm; (c) R=7 mm

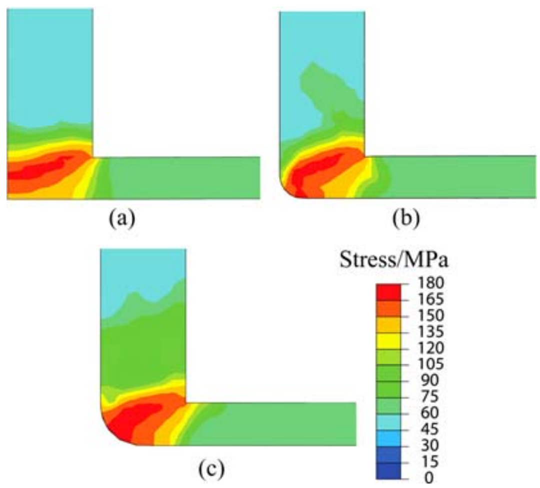

Fig. 5 Generalized stress distributions at deformation zone for r=0 and three different R values of R=0 (a), R=4 mm (b), R=7 mm (c)

It can be seen from Fig. 5 that for larger values of R, stress values greater than 150 MPa are induced in a slightly greater portion of the material in the deformation zone. This could be due to more uniform deformation pattern for greater values of R.

The velocity fields in the deformation zone for R values under consideration are illustrated in Fig. 6. It can be seen from this figure that for R=0 a dead-metal zone is formed in the outer corner of the die. By increasing the R value from 0 to 4 and then to 7, the dead-metal zone is gradually removed. Hence, considering an appropriate value of R in NECLE die design is very important. It is crucial when prevention of forming the dead-metal zone is essential. Therefore, this point should be considered in the die design, and appropriate die angles and corner radii should be selected.

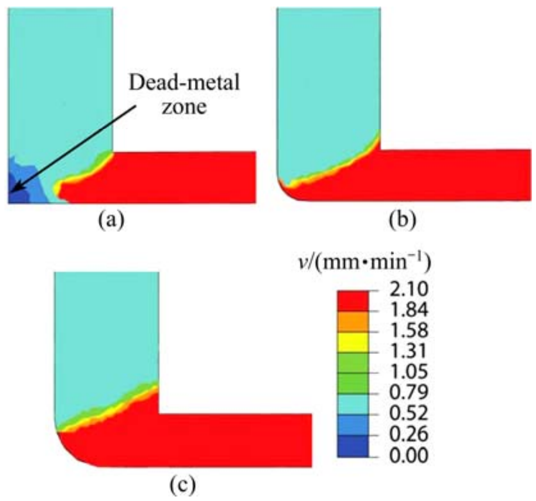

Fig. 6 Velocity field in deformation zone for r=0 and three various R values of R=0 (a), R=4 mm (b), R=7 mm (c)

4.1.2 Strain homogeneity of NECLE product

A homogeneous mechanical behavior is a point of interest in processes such as NECLE. To achieve this goal, both the inner and outer die radii should be selected carefully and appropriately. The effective strain distributions for different sets of r and R are illustrated in Fig. 7. The effective strain distribution is more uniform with the die corner radii pairs of (r=0, R=4 mm) and (r=4 mm, R=7 mm). The difference between the highest and lowest effective plastic strains (the range of strain values) in the horizontal channel can be used as a measure of homogeneity. The lower the difference, the more homogeneous the strain distribution is and, consequently, the more uniform the mechanical behavior of the product is. These differences for cases of (a), (b), (c) and (d) in Fig. 7 are 1.2, 0.23, 0.48 and 0.23, respectively. It is worth mentioning that a more homogeneous strain distribution is much more important than higher imposed plastic strain because it results in a greater uniformity of the produced structural components by means of this process.

The highest imposed plastic strains for different inner and outer radii are compared in Fig. 8. The maximum effective strain is achieved using inner and outer radii of r=4 mm and R=0. In this case, the inner radius has the greatest value (see Table 3) whereas the outer radius is the lowest. It can be seen in Fig. 8 that the next three higher values of plastic strain occurred in the case of R=0. Therefore, small outer radius in NECLE process plays an essential role in imposing higher plastic strains. In other words, by maintaining the r value

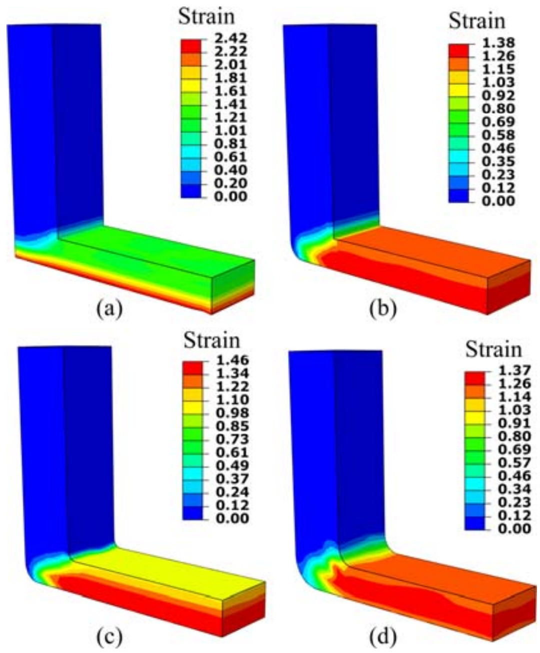

Fig. 7 Generalized plastic strain distribution at 250°C, v= 1 mm/min and different die corner radii of r=0, R=0 mm (a), r=0, R=4 mm (b), r=2, R=4 mm (c) and r=4, R=7 mm (d)

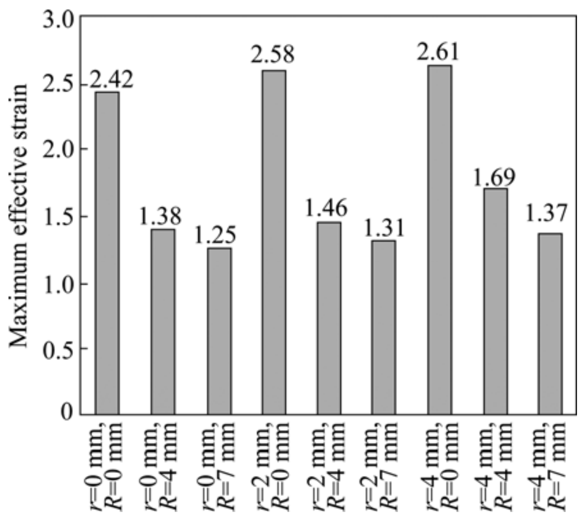

Fig. 8 The maximum effective strain for different inner and outer radii of die

constant, the maximum induced plastic strain reduces with increasing the R value. Another distinct pattern can be observed by maintaining the R value constant. For this case, the maximum imposed plastic strain increases with enlarging the r value.

The effective strain distributions in the steady zone of the horizontal channel (see Fig. 3(a), section $A-A$) and perpendicular to the extrusion direction are illustrated in Fig. 9 for different inner and outer corner radii. The horizontal axis is the distance from the bottom of the horizontal channel divided by the height of this channel, namely the normalized distance. The homogeneity of the induced effective strain in the product can be examined based on this figure. One can conclude from the figure that the three pairs of the die corner radii (r=0, R=0), (r=2 mm, R=0) and (r=4 mm, R=0) resulted in the most inhomogeneous strain distribution in the transverse section of the product. In the all these three sets, the inner radius is larger than or equal to the outer radius, and this could be the reason for the above-mentioned inhomogeneity.

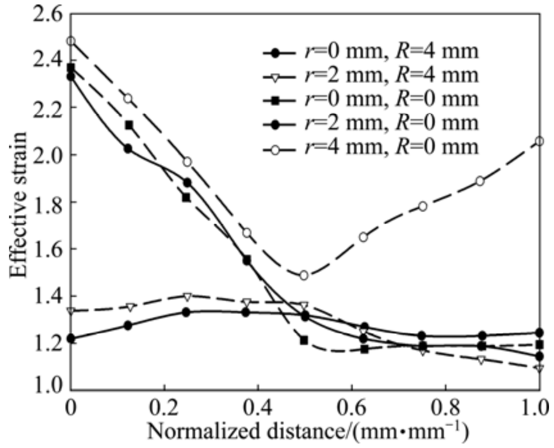

Fig. 9 Effective strain distributions through thickness of product (from bottom to top) for various sets of die radii

Figure 10 shows the micro-hardness profiles through the thickness of the products (along line B−B) from the bottom to the top surface. The hardness tests were carried out for steady deformation zones of the specimens processed with an NECLE die with r=0, R=4 mm and P/C=2 and different process parameters. The distance between each two following points was 0.5 mm and for each specimen, 13 points were selected in order to increase the accuracy of the hardness profile. All the profiles were almost smooth and with quite minor fluctuations. The difference between the minimum and maximum values of micro-hardness through each profile was less than 12%. Therefore, it can be concluded that by applying suitable die geometry for the NECLE process, a quite homogeneous steady zone can be provided for the product.

In addition to the strain distribution, the die fillet radii can affect the forming load. The forming load diagrams related to the strain contours illustrated in Fig. 7 are shown in Fig. 11. The steady values of forming load corresponding to t= 50 min are demonstrated in Fig. 12 for different pairs of r and R. Since for these simulations the ram velocity is equal to 1 mm/min, the displacement at t=50 min is nearly equal to 50 mm. It can be observed from Fig. 12 that the highest and lowest forming loads relate to r=2 mm, R=0 mm and r=0, R= 4 mm, respectively.

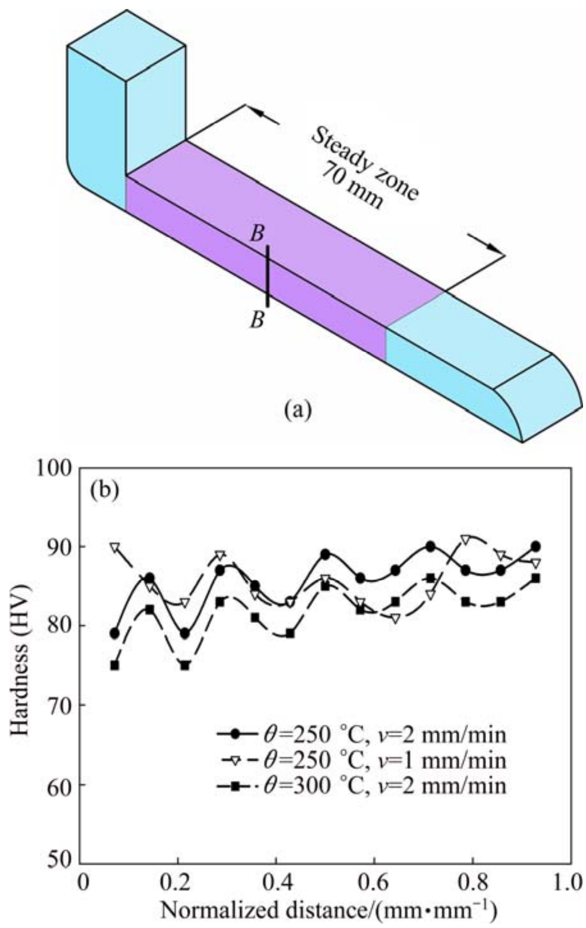

Fig. 10 Schematic diagram of specimen's steady deformed zone (a) and micro-hardness profile (b) through thickness of products deformed under different process conditions and NECLE die with r=0, R=4 mm and P/C=2

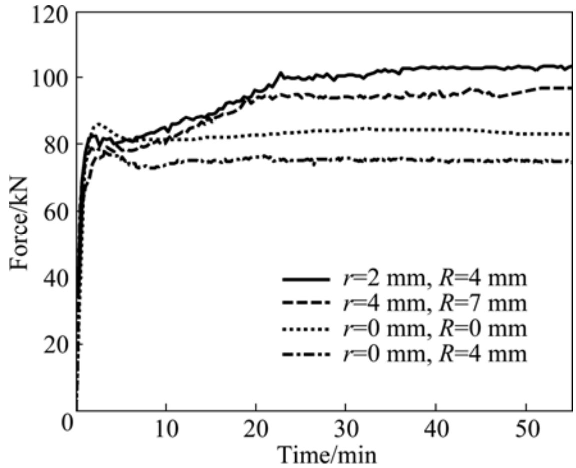

Fig. 11 FE forming loads obtained from simulations of NECLE with different die geometries based on Eulerian method

It can be seen from Fig. 11 that the forming load increases sharply during the initial stage of the NECLE process. Afterwards, it becomes steady and, hence, assuming the NECLE process as a steady-state operation by ignoring the initial stage of deformation is valid.

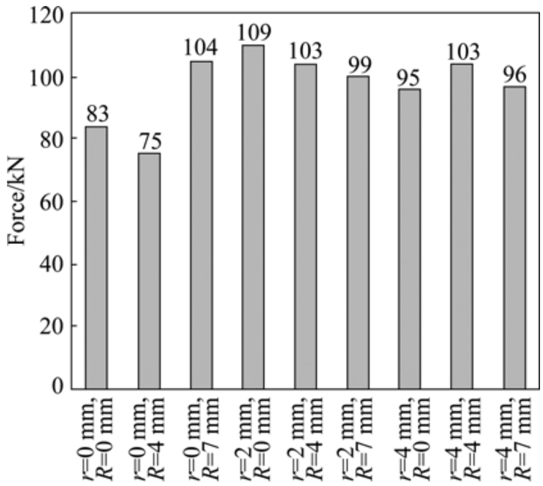

Fig. 12 Steady forming loads at t=50 min (displacement=50 mm) for NECLE operations with various sets of die radii

4.2 Effects of die angle

The corner angle (ϕ) of the die has an important effect on the forming load and flow pattern in an NECLE process. To investigate the influence of this variable on the process, other geometrical parameters were assumed to be r=0, R=4, P/C=2 mm. The process parameters were the same as those mentioned at the beginning of this section. To study the effects of the die angle on the deformation pattern, two different angles of 90° and 120° were considered. The effective strain and stress distributions are shown in Fig. 13 and Fig. 14, respectively. The maximum imposed plastic strain for the die angle of 90° is 1.38. By increasing the die angle, a lower peak effective strain of 0.98 has been resulted in. The reason for this 60% reduction is that the grains in the deformation zone are subjected to a greater shear deformation and larger changes in their orientations when a smaller die angle is involved. Therefore, the induced plastic strain is larger for the smaller corner angle of the die. Quite similar results were reported for the ECLE process [8,14]. PATIL-BASAVARAJ et al [14] stated that the strain homogeneity in ECLE process

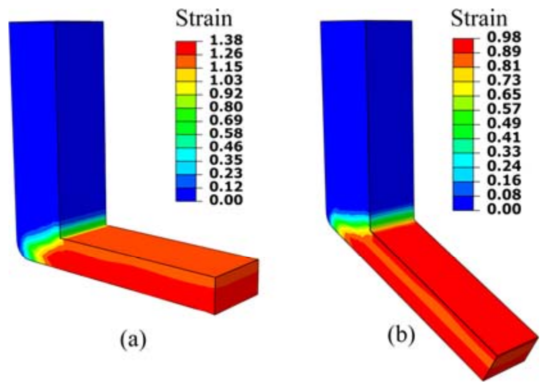

Fig. 13 Effective strain distributions for r=0, R=4 and two different die corner angles of ϕ=90° (a) and ϕ=120° (b)

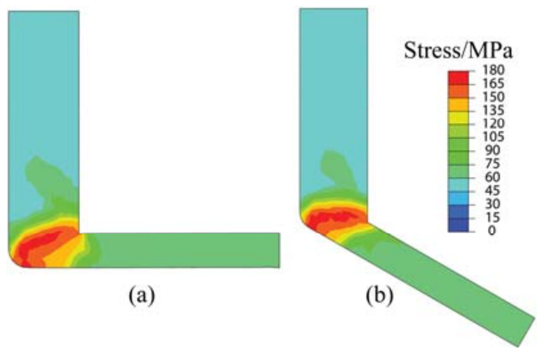

Fig. 14 Distribution of effective stress in sample for r=0, R=4 mm and two die angles of ϕ=90° (a), ϕ=120° (b)

increased with increasing the die corner angle. As it can be observed from Fig. 15, for both the corner angles in the NECLE process the effective strain distributions are almost uniform but with a higher strain for the smaller angle.

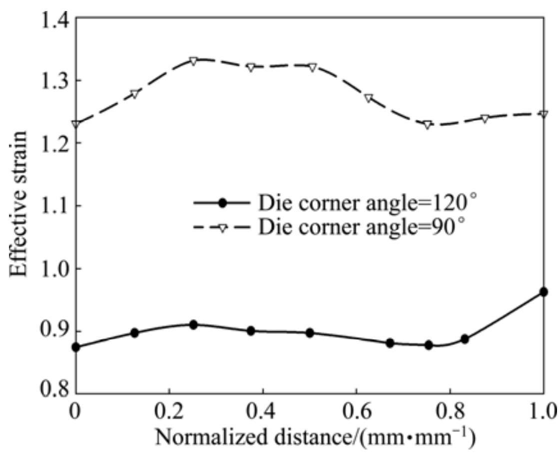

Fig. 15 Effective strain distributions through thickness of product (from bottom to top) for two different die corner angles

The die corner angle can also affect the forming load. The required forming loads for two different die angles and the relevant experimental load curve are compared in Fig. 16. By increasing the angle from 90° to 120°, the required forming load at 50 min (displacement=50 mm) reduced by about 14%. Hence, a die with a larger corner angle has longer useful life because it is subjected to smaller loads and pressures.

4.3 Effects of extrusion ratio

The effects of the extrusion ratio on the material flow were studied both numerically and experimentally. With this regard, the NECLE process was compared with ECLE operation. As mentioned earlier, in an ECLE process, the entry channel width (P) is equal to the thickness of the exit channel (C). Therefore, cross-sectional area remains constant, in contrary to NECLE operation. Hence, in addition to severe shear deformation at the junction of two channels, NECLE includes certain changes in the cross section of the product. Therefore, a higher plastic work is performed on the test sample.

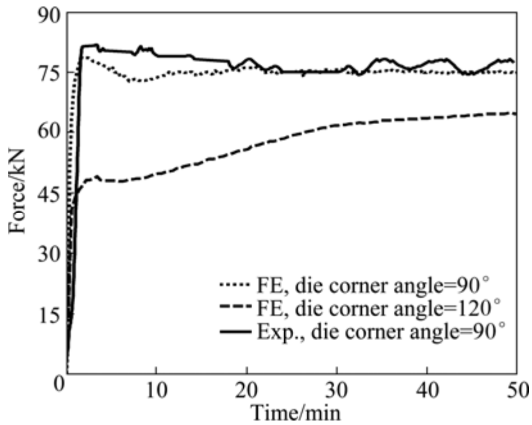

Fig. 16 Effects of die angle on forming load of NECLE process of AZ80 Mg alloy

TÓTH et al [6] proposed Eq. (1) to calculate the theoretical equivalent von Mises strain by the simple shear theory. This equation is suggested for a die angle of ϕ=90°:

$$\varepsilon=\left(\frac{P}{C}+\frac{C}{P}\right)/\sqrt{3} \tag{1}$$

where P/C is the extrusion ratio. For ECLE process, we have P/C=1 and, consequently, ε=1.16. In the present research work, two other values were assumed for P/C, namely P/C=1.5, 2 and, hence, the plastic strain values based on Eq. (1) were expected to be 1.25 and 1.44, respectively. This equation predicts 25% higher plastic strain for P/C=2 in comparison with P/C=1, namely, the average plastic strain in the NECLE process when consideration is expected to be higher than ECLE process. The effective strain distributions for P/C=2, 1.5 and 1 are shown in Fig. 17. The peak strain for P/C=2 is also very close to that estimated by Eq. (1). The predicted and FE values of this parameter are 1.44 and 1.38 for P/C=2, 1.25 and 1.41 for P/C=1.5, and 1.16 and 1.46 for P/C=1, respectively. It can be observed that the induced effective strains in the case of P/C=1.5, 1 are higher than P/C=2. The major cause of this higher effective strain is that the die geometry was optimized for P/C=2, and hence, with the employed set of die geometrical parameters a more homogeneous strain distribution is expected for P/C=2 as shown in Fig. 18. Although the maximum effective strains for P/C=1 and 1.5 are greater than the relevant average values predicted by Eq. (1), there is reverse situation for P/C=2. Therefore, the after-process properties of the test samples are expected to be better in the case of P/C=2 in comparison with ECLE (ECAP) process by using the optimal set of geometrical parameters.

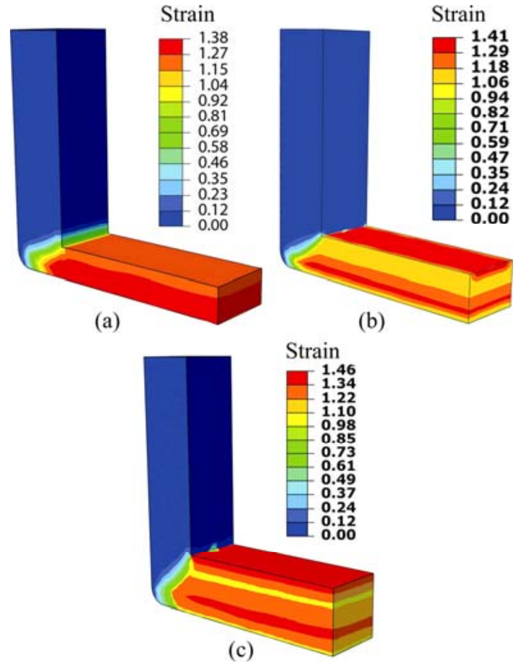

Fig. 17 Effective strain distributions for r=0, R=4 mm and three different extrusion ratios: (a) P/C =2; (b) P/C =1.5; (c) P/C=1

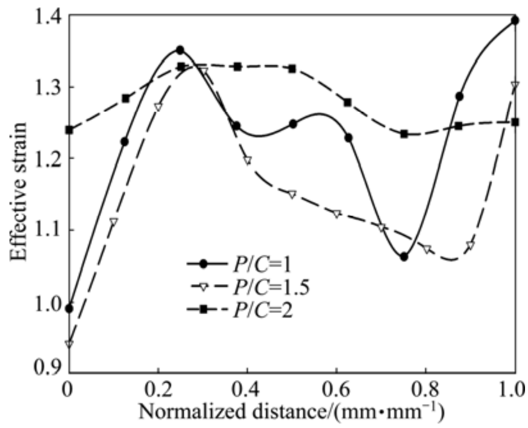

Fig. 18 Effective strain distributions for various extrusion ratios

The effective strain variations for P/C=2 and 1.5 at v=2 mm/min and two different temperatures of 250 and 300 °C are illustrated in Fig. 19. It can be seen that for both extrusion ratios, the maximum induced effective strain slightly increased by increasing the process temperature. However, the strain distribution is almost very similar in these cases.

The extrusion ratio can also affect the necessary forming load for the process. It is clear from Fig. 20 that the forming load for NECLE process with P/C=2 is higher than the related one for P/C=1.5. It can also be observed that there is a good agreement between the experimental and FE based load curves.

4.4 Comparison between FE and experimental results

Typical samples produced by means of the experiment and FE simulation are demonstrated in

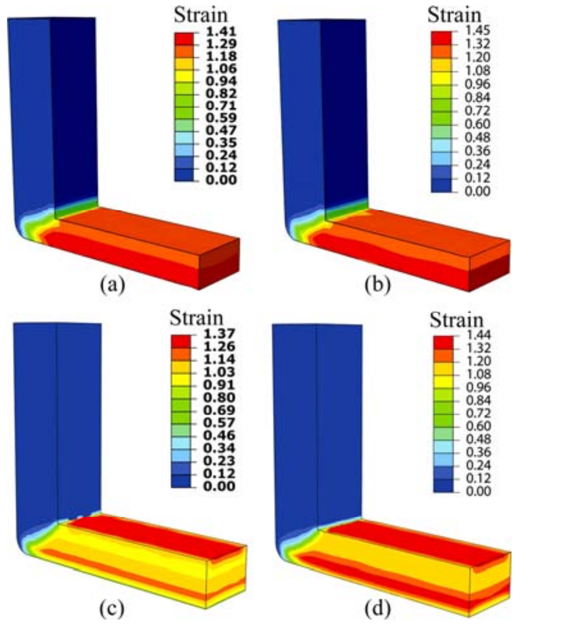

Fig. 19 Effective strain variations for r=0, R=4 mm, v=2 mm/min and P/C=2, θ=250 °C (a), P/C=2, θ=300 °C (b), P/C=1.5, θ=250°C (c), and P/C=1.5, θ=300°C (d)

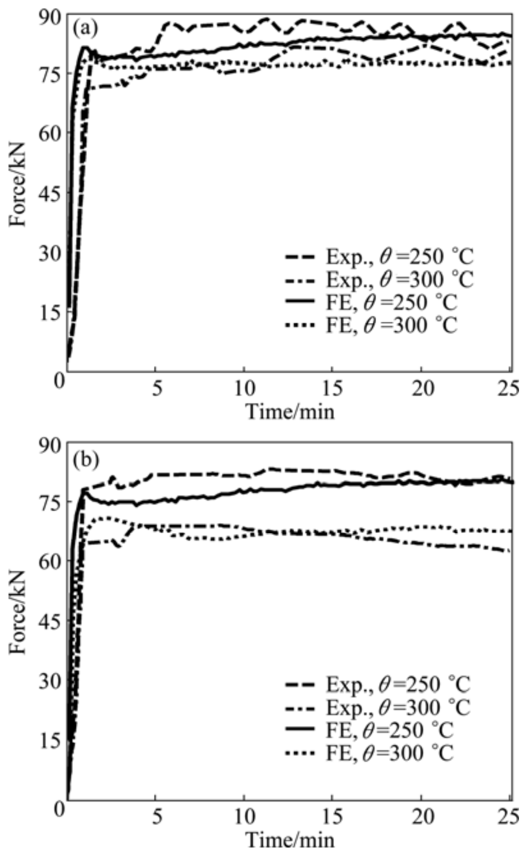

Fig. 20 Comparison between experimental and FE based load curves for r=0, R=4 mm, v=2mm/min for two extrusion ratios of P/C=2 (a) and P/C=1.5 (b)

Fig. 21. It can be seen that these samples are fairly alike and the FE simulations could reasonably predict the shape of the final sample. The experimental and FE based load curves are also compared in Fig. 22. The FE load−displacement curve illustrated in Fig. 22 corresponds to the ALE method explained in section 2.2.1. On the other hand, the load curve obtained from the steady state simulation is also plotted against the time (Fig. 22). The load values of both the simulations are quite in good agreement with the experimental findings. Almost all of these curves end to an approximate load of 80 kN in the steady region of the curve. The small deviations between the experimental and the FE load curves can be attributed to some reasons such as the complexity of the process and the complicated material behavior, which is quite difficult to model. Other sources of error might be inaccuracy in the evaluation of the flow stress of AZ80 alloy and estimation of the friction factor at the tool−workpiece interface. Slight formation of flash in the practical NECLE tests could also cause some deviations from the FE findings.

Fig. 21 Experimental specimen (at top) together with deformed FE model

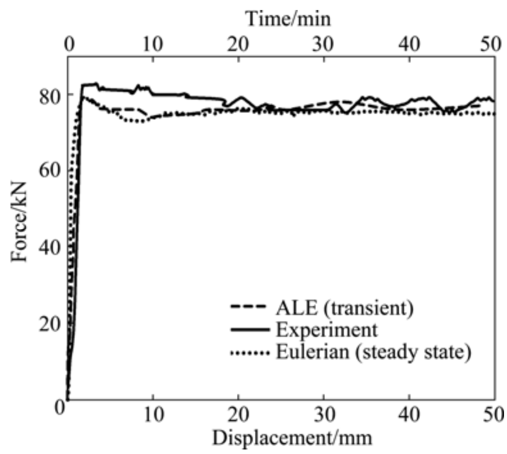

Fig. 22 Experimental load curves with FE based findings resulted from ALE and Eulerian methods

5 Conclusions

1) The out radium R has an important role in the formation of the dead-metal zone. It is possible to prevent creation of this zone by increasing the outer corner radius.

2) An appropriate selection of the inner and outer radii of the die has an important role in homogeneity of the imposed effective strain and, consequently, the final

product. For instance, in the case of r=0 and R=4 mm, more homogeneous strain distribution was achieved in comparison with other sets of die corner radii. The maximum plastic strain in the product was observed in the case of r=4 and R=0, i.e. a significantly larger value of inner radius in comparison with the outer radius.

3) While maintaining the die outer radius (R) constant, the maximum imposed plastic strain in the product is increased with increasing the inner corner radius (r).

4) Smaller corner angles of the die result in higher levels of deformation as well as larger forming loads. The gradient of the material properties of the product is also higher for smaller die angles. Despite the average strain values, the homogeneities of strain variation for two die angles of 90° and 120° are similar.

5) A higher extrusion ratio leads to higher effective strains in the product. Therefore, the induced plastic strain in a single pass is higher in a NECLE operation compared with corresponding ECLE process with an extrusion ratio of 1.

6) With a suitable set of geometrical parameters, a uniform strain distribution with a higher average strain in comparison with ECLE process could be achieved by using the NECLE operation.

7) The maximum effective strains obtained from the FE analyses of the NECLE process of AZ80 alloy at various conditions are in good correlation with the strains estimated by $\varepsilon=\left(\dfrac{P}{C}+\dfrac{C}{P}\right)/\sqrt{3}$.

References

[1] CHOI H, CHOI J, HWANG B. The forming characteristics of radial-backward-extrusion [J]. Journal of Materials Processing Technology, 2001, 113: 141−147.

[2] SEGAL V, REZNIKOV V, DROBYSHEVSKIY A, KOPYLOV V. Plastic working of metals by simple shear [J]. Russian Metallurgy, 1981, 1: 99−105.

[3] ZUYAN L, GANG L, WANG Z. Finite element simulation of a new deformation type occurring in changing-channel extrusion [J]. Journal of Materials Processing Technology, 2000, 102: 30−32.

[4] OHASHI T, HAYASHI K. Lateral extrusion of A6063 aluminum alloy pipes with a lost core [J]. Journal of Materials Processing Technology, 2003, 138: 560−563.

[5] TALEBANPOUR B, EBRAHIMI R, JANGHORBAN K. Microstructural and mechanical properties of commercially pure aluminum subjected to dual equal channel lateral extrusion [J]. Materials Science and Engineering A, 2009, 527: 141−145.

[6] TÓTH L, LAPOVOK R, HASANI A, GU C. Non-equal channel angular pressing of aluminum alloy [J]. Scripta Materialia, 2009, 61: 1121−1124.

[7] YOON S, QUANG P, HONG S, KIM H. Die design for homogeneous plastic deformation during equal channel angular pressing [J]. Journal of Materials Processing Technology, 2007, 187−188: 46−50.

[8] HU H, ZHANG D, PAN F. Die structure optimization of equal channel angular extrusion for AZ31 magnesium alloy based on finite element method [J]. Transactions of Nonferrous Metals Society of China, 2010, 20: 259−266.

[9] ZHANG C, ZHAO G, CHEN H, GUAN Y, KOU F. Numerical simulation and metal flow analysis of hot extrusion process for a complex hollow aluminum profile [J]. International Journal of Advanced Manufacturing Technology, 2012, 60: 101−110.

[10] BELYTSCHKO T, LIU W, MORAN B. Nonlinear finite elements for continuum and structures [M]. New York: Wiley Interscience, 2000.

[11] van LEER B. Towards the ultimate conservative difference scheme IV: A new approach to numerical convection [J]. Journal of Computational Physics, 1977, 23: 276−299.

[12] BENSON D. Momentum advection on a staggered mesh [J]. Journal of Computational Physics, 1977, 100: 143−162.

[13] HIBBITT D. ABAQUS analysis user's manual [M]. Version 6.7. Rhode Island: Karlsson and Sorenso Inc, 2007.

[14] PATIL-BASAVARAJ V, CHAKKINGAL U, PRASANNA-KUMAR T. Study of channel angle influence on material flow and strain inhomogeneity in equal channel angular pressing using 3D finite element simulation [J]. Journal of Materials Processing Technology, 2009, 209: 89−95.

[15] GOUVEIA B, RODRIGUES J, MARTINS P. Steady-state finite-element analysis of cold forward extrusion [J]. Journal of Materials Processing Technology, 1998, 73: 281−288.

[16] FERESHTEH-SANIEE F, BARATI F, BADNAVA H, FALLAH-NEJAD K H. An exponential material model for prediction of the flow curves of several AZ series magnesium alloys in tension and compression [J]. Materials & Design, 2012, 35: 1−11.

[17] FERESHTEH-SANIEE F, BADNAVA H, PEZESHKI-NAJAFABADI M. Application of T-shape friction test for AZ31 and AZ80 magnesium alloys at elevated temperatures [J]. Materials & Design, 2011, 32: 3221−3230.

模具几何形状对 AZ80 镁合金非等通道横向挤压的影响

Faramarz FERESHTEH-SANIEE[1], Mohammad ASGARI[1], Mahmoud BARATI[2], Sayed Mahmoud PEZESHKI[1]

1. Mechanical Engineering Department, Faculty of Engineering, Bu-Ali Sina University, Hamedan, Iran;
2. Applied Mechanics Department, Faculty of Mechanical Engineering, K.N. Toosi University of Technology, Tehran, Iran

摘　要：非等通道横向挤压(NECLE)是一种新工艺, 与等通道横向挤压(ECLE)相比，采用非等通道横向挤压工艺可以得到更加细化的晶粒。对该模具设计工艺进行了数值模拟和实验研究。发现数值模拟和实验结果之间存在良好的相关性, 并进行了全面的有限元分析。考虑了不同的模具几何参数，并研究了这些参数对诱导塑性应变、应力分布、速度场和载荷的影响。结果表明，当具有一组合适的模具几何参数时，与等通道横向挤压相比，采用非等通道横向挤压工艺可以得到高诱导有效应变和更均匀应变分布。

关键词：镁合金；非等通道横向挤压；模具几何形状；均匀性；任意 Lagrangian−Eulerian 法

(Edited by Xiang-qun LI)